

PYROLYSIS OF A BINARY HYDROCARBON MIXTURE: REACTION MODELING

PHILLIP E. SAVAGE

DEPARTMENT OF CHEMICAL ENGINEERING
UNIVERSITY OF MICHIGAN
ANN ARBOR, MI 48109

INTRODUCTION

Numerous pyrolyses of coal model compounds (e.g., refs 1-5) have provided substantial insight into the thermal reactions of the moieties they mimicked. The results of experiments with single compounds, however, provide no information about the interactions that can occur between the distinct chemical components in complex reactants such as coal. Because an active center (e.g., free radical) derived from one chemical moiety can react with a second, different moiety, reaction pathways that are important for the pyrolysis of a single model compound might not be equally important for the model-compound-like moiety in a coal macromolecule. Conversely, pathways unobserved in single-component pyrolyses might be operative in coal pyrolysis.

Previous reports of the pyrolysis of binary mixtures of high-molecular-weight compounds, though few (6), demonstrated that reactions between active centers derived from the two different compounds or between an active center from one compound and the second compound itself can affect the reaction rates, product selectivities, and reaction pathways. Zhou and Crynes (7), for example, pyrolyzed isomeric ethylphenols in dodecane and found that ethylphenol inhibited the rate of dodecane cracking and that dodecane accelerated the rate of ethylphenol conversion. They postulated that the interactions between the ethylphenol-derived and dodecane-derived radicals were considerable and were responsible for the differences between the pure compound and copyrolysis results. Allen and Gavalas (8) reported that the rate of decomposition of methylene and ether bridges in coal model compounds was enhanced when the compounds were pyrolyzed in 1,2-dihydronaphthalene (dialin). They suggested that an aromatic displacement reaction with atomic hydrogen (formed from dialin decomposition) was responsible for the accelerated bridge decomposition.

To gain additional insight into the pyrolysis of binary mixtures of high-molecular-weight compounds, a reaction model has been developed to simulate the copyrolysis of tetradecylbenzene (TDB) and dodecylcyclohexane (DDC). These compounds mimic alkylaromatic and alkylnaphthenic moieties in coal and asphaltenes.

REACTION MODEL

The essential features of the free-radical pyrolysis of both long-chain alkylbenzenes and alkylcyclohexanes can be modeled as three parallel chains coupled via chain transfer steps (9-11). These three chains arise because there are only three types of aliphatic carbons in TDB and in DDC that exhibit unique reactivities. In TDB, hydrogen abstraction at the α carbon leads to a resonance-stabilized, secondary benzylic radical whereas abstraction at all other positions produces a less stable secondary alkyl radical. Thus the α carbon possesses unique kinetics in the hydrogen abstraction step. Unique among the non- α radicals in TDB, the γ radical leads to a resonance-stabilized, primary benzyl radical upon β -scission, whereas β -scission of all other TDB radicals produces a primary alkyl radical. Thus β -scission of the γ radical is the fastest decomposition step. All non- α and non- γ positions in TDB share roughly equal reactivities for hydrogen abstraction and β -scission and therefore collectively constitute the third category.

Similar to the influence of the aromatic ring and the resultant preferential formation of benzylic radicals in TDB, the naphthenic ring in DDC affords preferential formation of tertiary radicals in hydrogen abstraction steps and secondary radicals in β -scission steps. Hydrogen abstraction at the ring carbon bearing the aliphatic chain, which produces a tertiary DDC radical, is the fastest abstraction step because abstraction

at all other positions yields less stable secondary radicals. β -scission of the β -DDC radical, which produces a secondary cyclohexyl radical is the unique decomposition step because all other β -scission steps lead to primary alkyl radicals. All non- β and non-tertiary positions in DDC share roughly equal reactivities for both hydrogen abstraction and β -scission.

The previously discerned (9-11) elementary reaction steps for neat pyrolysis of TDB and DDC, summarized in Figure 1, include a single initiation step and termination by all possible radical recombinations. R denotes a reactant molecule, and the superscripts A and B refer to TDB and DDC, respectively. Following standard notation, μ radicals are those that participate in unimolecular propagation steps, and β radicals propagate chain reactions via bimolecular steps. Table I provides the chemical identities of the species in Figure 1.

Pyrolysis proceeds via the three parallel chain reactions in the center column of Figure 1 to produce β_1 H plus Q_1 , β_2 H plus Q_2 , and β_3 H plus Q_3 as the major products. Chain transfer, depicted in the two peripheral columns, can occur via both μ and β radicals. The interaction steps take the form of a free radical derived from one compound abstracting hydrogen from the second compound and additional termination steps involving the recombination of radicals derived from the two different substrates. Note that the copyrolysis mechanism of Figure 1 depicts only the primary reactions.

KINETICS DEVELOPMENT

Reaction rate expressions were derived for TDB and DDC on the basis of the mechanism in Figure 1 by invoking the pseudo-steady-state and long-chain approximations (12,13). These approximations allow formulation of the algebraic β_i balance for compound A (TDB) as Equation 1,

$$r_{\beta_i}^A = 0 = k_{\mu_i}^A \mu_i^A - \sum_{j=1}^3 k_{ij}^{AA} \beta_j^A R^A - \sum_{j=1}^3 k_{ij}^{AB} \beta_j^A R^B \quad (1)$$

and this permits solution for μ_i^A as

$$\mu_i^A = y_i^A \beta_i^A \quad (2)$$

where

$$y_i^A = \frac{k_i^{AA} R^A + k_i^{AB} R^B}{k_{\mu_i}^A} \quad (3)$$

with $k_i^{AA} = \sum_{j=1}^3 k_{ij}^{AA}$ and $k_i^{AB} = \sum_{j=1}^3 k_{ij}^{AB}$.

Similarly, the β_i^B balance leads to

$$\mu_i^B = y_i^B \beta_i^B \quad (4)$$

where the expression for y_i^B can be obtained from Equation 3 by transposing the A and B superscripts.

The double subscript notation employed for the hydrogen abstraction rate constants identifies, respectively, the attacking radical and the resultant μ radical. The double superscript notation identifies, respectively, the substrate from which the attacking radical was derived and the substrate attacked. Primed and unprimed rate constants denote hydrogen abstraction from either of the substrates by μ and β radicals, respectively.

The long-chain, steady-state μ_i^A balance is given as Equation 5.

$$r_{\mu_i}^A = 0 = \sum_{j=1}^3 k_{ji}^{AA} \beta_j^A R^A - k_{\mu_i}^A \mu_i^A - \sum_{j=1 \neq i}^3 k_{ij}^{AA} \mu_j^A R^A + \sum_{j=1 \neq i}^3 k_{ji}^{AA} \mu_j^A R^A - \sum_{j=1}^3 k_{ij}^{AB} \mu_i^A R^B + \sum_{j=1}^3 k_{ji}^{BA} \mu_j^B R^A + \sum_{j=1}^3 k_{ji}^{BA} \beta_j^B R^A \quad (5)$$

The balance for μ_i^B is completely analogous and can be obtained by transposing the A and B superscripts in Equation 5.

Substituting Equations 2 and 4 for the concentrations of the μ_i^A and μ_i^B radicals, respectively, into Equation 5 leads, after considerable rearrangement, to Equation 6.

$$\sum_{j=1 \neq i}^3 Z_{ji}^{AA} \beta_j^A + \sum_{j=1}^3 Z_{ji}^{BA} \beta_j^B = \beta_i^A \left(\sum_{j=1 \neq i}^3 Z_{ij}^{AA} + \frac{R^B}{R^A} \left(\sum_{j=1}^3 Z_{ij}^{AB} \right) \right) \quad (6)$$

where

$$Z_{ij}^{AA} = k_{ij}^{AA} + y_i^A k_{ij}^{AA} \quad (7)$$

$$Z_{ij}^{BA} = k_{ij}^{BA} + y_i^B k_{ij}^{BA} \quad (8)$$

Expressions for Z_{ij}^{BB} and Z_{ij}^{AB} can be obtained from Equations 7 and 8, respectively, by transposing their superscripts.

Equation 6 and the analogous set of equations for substrate B provide five independent equations in the six unknowns β_i^A and β_i^B . Thus a balance on the total radical population must be written to solve for the individual radical concentrations and ultimately the reaction rate. The free radical concentration changes only as a result of initiation and termination steps, thus applying the pseudo-steady-state approximation to the net rate of radical production results in equating the rates of initiation and termination.

Since both theory and experimental evidence suggest that rate constants for radical recombinations are typically $10^{9.0 \pm 0.5}$ l/mol-s (14,15), all termination rate constants were taken to be equal except for the statistical factor (16) that renders the rate constant for combination of two identical radicals, ω_T , one-half that for two dissimilar species. This approximation combines with the initiation and termination steps depicted in Figure 1 to give Equation 9 as the steady-state radical balance.

$$\alpha_f^A R^A + \alpha_f^B R^B = \omega_T \left[\sum_{i=1}^3 (\mu_i^A + \mu_i^B + \beta_i^A + \beta_i^B) \right]^2 \quad (9)$$

Eliminating μ_i^A and μ_i^B from Equation 9 via Equations 2 and 4, respectively, gives Equation 10.

$$\left[\frac{\alpha_f^A R^A + \alpha_f^B R^B}{\omega_T} \right]^{1/2} = \sum_{i=1}^3 \left[\beta_i^A (1 + y_i^A) + \beta_i^B (1 + y_i^B) \right] \quad (10)$$

This equation, Equation 6, and analogous expressions for substrate B were solved numerically for the β radical concentrations with estimated rate constants as parameters. Table II summarizes the Arrhenius parameter estimates used in the reaction model. These values are representative of literature estimates (1,2,14,15,17-22) for similar types of reactions.

The reaction rates were then determined from the long-chain rate expressions below.

$$-r_A = R^A \sum_{i=1}^3 \left[\beta_i^A (k_i^{AA} - \frac{R^B}{R^A} k_i^{AB} y_i^A) + \beta_i^B (k_i^{BA} + k_i^{BA} y_i^B) \right] \quad (11)$$

$$-r_B = R^B \sum_{i=1}^3 \left[\beta_i^B (k_i^{BB} - \frac{R^A}{R^B} k_i^{BA} y_i^B) + \beta_i^A (k_i^{AB} + k_i^{AB} y_i^A) \right] \quad (12)$$

Relative rates for DDC and TDB pyrolysis were calculated as the ratio of the rate at a given value of [TDB]/[DDC] (or [DDC]/[TDB]) to the rate calculated for the pyrolysis of the pure compound.

RESULTS AND DISCUSSION

Figure 2 displays the relative rates calculated for DDC and TDB pyrolysis at 400°C as functions of the absolute concentration of substrate and the relative concentrations of the two components.

At a DDC concentration of 0.001M, the addition of small quantities of TDB accelerated DDC pyrolysis, and the relative rate reached a maximum value of 1.14. Further additions of TDB inhibited the rate, and it decreased to a minimum value of 1.06. Interestingly, upon continued addition, TDB again accelerated DDC pyrolysis. At $[DDC] = 0.01M$, TDB initially accelerated the rate, and a maximum value of 1.28 was attained. Additional quantities of TDB reduced the relative rate. A maximum relative rate was also observed at $[DDC] = 0.10M$. In this case the maximum value was 1.10 at a $[TDB]/[DDC]$ ratio of 0.0158. When $[DDC] = 1.00M$, however, TDB acted only as an inhibitor.

The results for simulated TDB pyrolysis in the presence of added DDC at 400°C show that DDC had little effect on the relative rate until high ($> 10^{-1}$) $[DDC]/[TDB]$ ratios were attained. At these high ratios, DDC accelerated TDB pyrolysis for $[TDB] = 0.001$ and $0.01M$. The addition of DDC had little ($< 0.3\%$) effect on TDB pyrolysis kinetics at the higher TDB concentrations.

These results clearly demonstrate that interactions occurring during the pyrolysis of a binary mixture of high-molecular-weight hydrocarbons can alter the apparent kinetics from those observed in pure component pyrolysis. They also show that inhibition and acceleration of reaction rates is a complex function of both the relative amounts of the two components as well as their absolute concentrations. For example, at a $[TDB]/[DDC]$ ratio of 0.05, TDB can either inhibit, accelerate, or have no effect on the relative rate of DDC disappearance depending on the DDC concentration.

ACKNOWLEDGEMENT

This work was supported in part by the University of Michigan Office of Energy Research.

LITERATURE CITED

1. Gilbert, K. E., Gajewski, F. J. *J. Org. Chem.*, **1982**, *47*, 4899.
2. Poutsma, M. L., Dyer, C. W. *J. Org. Chem.*, **1982**, *47*, 4903.
3. Panvelker, S. V., Shah, Y. T., Cronauer, D. C., *Ind. Eng. Chem. Fundam.*, **1982**, *21*, 236.
4. Benjamin, B. M., Raaen, V. F., Maupin, P. H., Brown, L. L., Collins, C. J., *Fuel*, **1978**, *57*, 269.
5. Cronauer, D. C., Jewell, D. M., Shah, Y. T., Modi, R. J., *Ind. Eng. Chem. Fundam.*, **1979**, *18*, 153.
6. Rebeck, C. in *Pyrolysis: Theory and Industrial Practice*, L. F. Albright, B. L. Crynes, W. H. Corcoran, Eds. Academic press **1983**.
7. Zhou, P., Crynes, B. L., *Ind. Eng. Chem. Process Des. Dev.*, **1986**, *25*, 898.
8. Allen, D. T., Gavalas, G. R. *Fuel*, **1984**, *63*, 586.
9. Savage, P. E., Klein, M. T., *Ind. Eng. Chem. Research* **1987**, *26*, 488.
10. Savage, P. E., Klein, M. T., *Ind. Eng. Chem. Research* submitted.
11. Savage, P. E., Klein, M. T., *Chem. Eng. Sci.* submitted.
12. Come, G., *J. Phys. Chem.*, **1977**, *81*, 2560.
13. Gavalas, G. R., *Chem. Eng. Sci.*, **1966**, *21*, 133.
14. Benson, S. W., *Thermochemical Kinetics*, John Wiley & Sons, New York **1976**.
15. Kochi, J. K., *Free Radicals*, John Wiley & Sons, New York **1973**.
16. Pryor, W. A., *Free Radicals*, McGraw-Hill **1966**.
17. Sundaram, K. W., Froment, G. F., *Ind. Eng. Chem. Fundam.*, **1978**, *17*, 174.
18. Kissin, Y. V., *Ind. Eng. Chem. Research*, **1987**, *26*, 1633.
19. Ranzi, E., Dente, M., Pierucci, S., Biardi, G., *Ind. Eng. Chem. Fundam.*, **1983**, *22*, 132.
20. Edelson, D., Allara, D. L., *Int. J. Chem. Kin.*, **1980**, *12*, 605.
21. Ebert, K. H., H. J. Ederer, and P. S. Schmidt, in *ACS Symposium Series No. 65*, V. W. Weekman and D. Luss, Eds. **1978**, 313.
22. Miller, R. E., Stein, S. E., *J. Phys. Chem.*, **1981**, *85*, 580.

TABLE I: IDENTITY OF SPECIES IN FIGURE 1 FOR TDB-DDC COPYROLYSIS

β_1^A	Benzyl Rad	μ_1^A	γ -TDB Rad	β_1^B	Cyclohexyl Rad	μ_1^B	β -DDC Rad
β_2^A	Dodecyl Rad	μ_2^A	α -TDB Rad	β_2^B	Undecyl Rad	μ_2^B	3°-DDC Rad
β_3^A	Non-TDB Rad	μ_3^A	Other TDB Rad	β_3^B	Non-DDC Rad	μ_3^B	Other DDC Rad
$\beta_1^A H$	Toluene	Q_1^A	Tridecene	$\beta_1^B H$	Cyclohexane	Q_1^B	Dodecene
$\beta_2^A H$	Dodecane	Q_2^A	Styrene	$\beta_2^B H$	Undecane	Q_2^B	Methylene Cyclohexane
$\beta_3^A H$	Minor Products	Q_3^A	Minor Products	$\beta_3^B H$	Minor Products	Q_3^B	Minor Products

TABLE II: RATE CONSTANT ESTIMATES FOR TDB-DDC COPYROLYSIS

Type of Reaction	log A (s^{-1} or $M^{-1}s^{-1}$)	E_A (kcal/mol)	Rate Constants
Initiation			
TDB	15.0	68.5	α_f^A
DDC	16.5	79.0	α_f^B
Termination			
	8.5	0	ω_T
β-scission*			
B	14.8	28.3	$k_{\mu_1}^A$
2°	13.0	28.5	$k_{\mu_2}^B$
1°	13.0	26.5	$k_{\mu_3}^A, k_{\mu_3}^B, k_{\mu_3}^B, k_{\mu_3}^B$
Hydrogen Abstraction**			
B + 2° H	8.5	18.5	$k_{21}^{A,B}, k_{11}^{A,A}, k_{13}^{A,A}, k_{21}^{A,A}, k_{23}^{A,A}, k_{23}^{A,B}$ $k_{11}^{A,B}, k_{13}^{A,B}$
B + 3° H	8.5	17.0	$k_{22}^{A,B}, k_{12}^{A,B}$
B + B H	8.5	14.0	$k_{12}^{A,A}$
3° + 2° H	8.5	14.5	$k_{21}^{B,B}, k_{23}^{B,B}, k_{21}^{B,A}, k_{23}^{B,A}$
3° + B H	8.5	10.0	$k_{22}^{B,A}$
2° + 2° H	8.5	12.5	$k_{13}^{A,A}, k_{31}^{A,A}, k_{11}^{B,B}, k_{13}^{B,B}, k_{13}^{B,B}, k_{31}^{B,B}, k_{11}^{A,B}, k_{13}^{A,B}$ $k_{13}^{A,B}, k_{31}^{A,B}, k_{33}^{A,B}, k_{31}^{B,A}, k_{33}^{B,A}, k_{11}^{B,A}, k_{13}^{B,A}$ $k_{11}^{B,A}, k_{13}^{B,A}$
2° + 3° H	8.5	11.0	$k_{12}^{B,B}, k_{12}^{B,B}, k_{32}^{B,B}, k_{12}^{A,B}, k_{32}^{A,B}$
2° + B H	8.5	8.0	$k_{12}^{A,A}, k_{32}^{A,A}, k_{12}^{A,A}, k_{32}^{A,A}, k_{12}^{B,A}$
1° + 2° H	8.5	10.5	$k_{21}^{A,A}, k_{23}^{A,A}, k_{31}^{A,A}, k_{33}^{A,A}, k_{21}^{B,B}, k_{23}^{B,B}, k_{31}^{B,B}$ $k_{21}^{A,B}, k_{23}^{A,B}, k_{33}^{A,B}, k_{31}^{A,B}, k_{21}^{A,B}, k_{23}^{A,B}, k_{31}^{A,B}$ $k_{31}^{B,A}, k_{33}^{B,A}$
1° + 3° H	8.5	9.0	$k_{22}^{B,B}, k_{32}^{B,B}, k_{22}^{A,B}, k_{32}^{A,B}$
1° + B H	8.5	6.0	$k_{22}^{A,A}, k_{32}^{A,A}, k_{22}^{B,A}, k_{32}^{B,A}$

* Reactions indicate type of radical produced (B - Benzyl, 2° - Secondary, 1° - Primary)

** Reactions indicate type of abstracting radical and type of hydrogen abstracted, respectively

FIGURE 1: TDB-DDC PRIMARY COPYROLYSIS MECHANISM

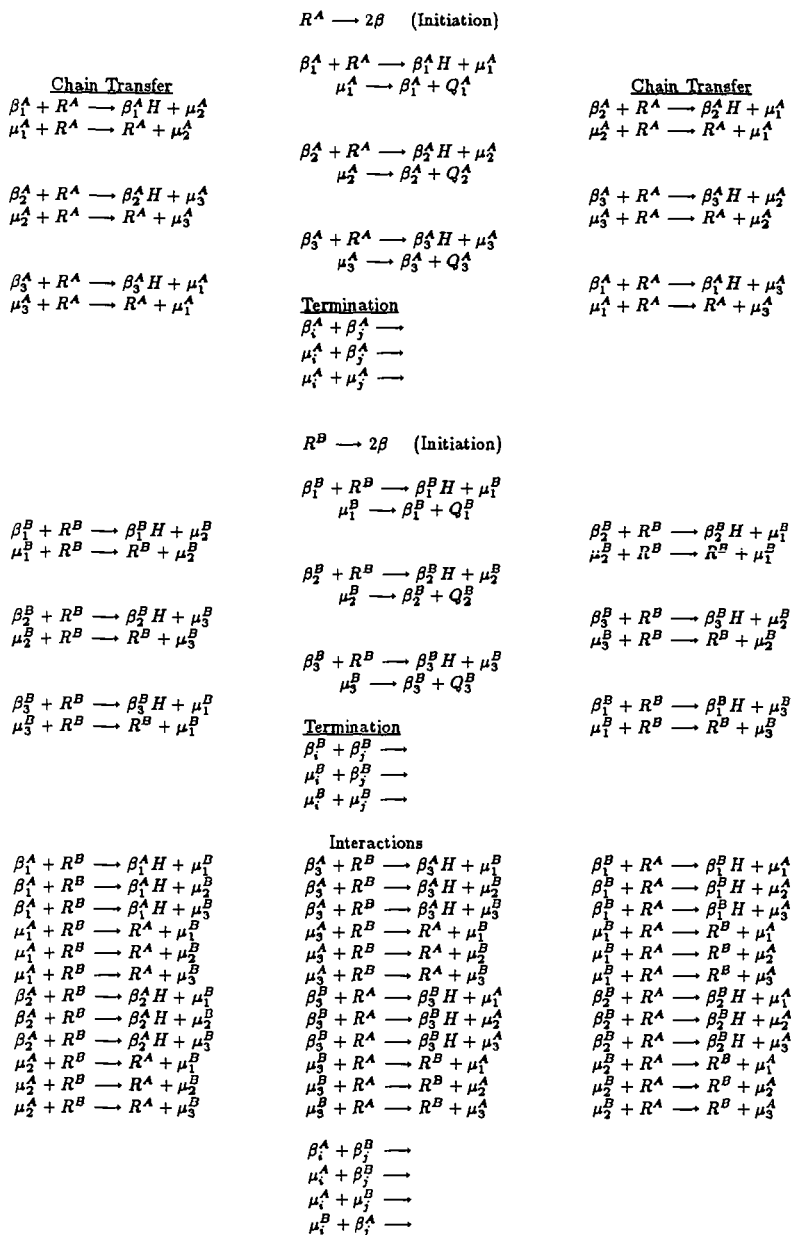
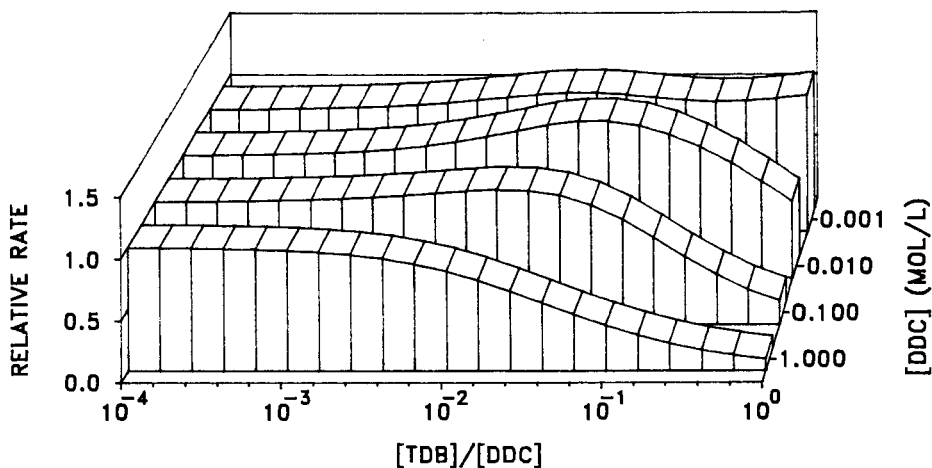


FIGURE 2: DDC-TDB COPYROLYSIS SIMULATION
RELATIVE RATE FOR DDC



RELATIVE RATE FOR TDB

